

## GRAVITATIONAL SETTLING OF $^{22}\text{Ne}$ AND WHITE DWARF EVOLUTION

E. GARCÍA-BERRO<sup>1</sup>

Departament de Física Aplicada, Escola Politècnica Superior de Castelldefels, Universitat Politècnica de Catalunya,  
Avenida del Canal Olímpic, s/n, 08860 Castelldefels, Spain; garcia@fa.upc.edu

L. G. ALTHAUS<sup>2</sup> AND A. H. CÓRSICO<sup>2</sup>

Facultad de Ciencias Astronómicas y Geofísicas, Universidad Nacional de La Plata, Paseo del Bosque s/n,  
(1900) La Plata, Argentina; althaus@fcaglp.unlp.edu.ar, acorsico@fcaglp.unlp.edu.ar

AND

J. ISERN<sup>1</sup>

Institut de Ciències de l'Espai, CSIC, Facultat de Ciències, Campus UAB,  
08193 Bellaterra, Spain; isern@ieec.fcr.es

Received 2007 September 3; accepted 2007 December 6

### ABSTRACT

We study the effects of the sedimentation of the trace element  $^{22}\text{Ne}$  in the cooling of white dwarfs. In contrast with previous studies—which adopted a simplified treatment of the effects of  $^{22}\text{Ne}$  sedimentation—this is done self-consistently for the first time, using an up-to-date stellar evolutionary code in which the diffusion equation is coupled with the full set of equations of stellar evolution. Due to the large neutron excess of  $^{22}\text{Ne}$ , this isotope rapidly sediments in the interior of the white dwarf. Although we explore a wide range of parameters, we find that when using the most reasonable assumptions concerning the diffusion coefficient and the physical state of the white dwarf interior, the delay introduced by the ensuing chemical differentiation is minor for a typical  $0.6 M_{\odot}$  white dwarf. For more massive white dwarfs, say  $M_{\text{WD}} \sim 1.0 M_{\odot}$ , the delay turns out to be considerably larger. These results are in qualitatively good accord with those obtained in previous studies, but we find that the magnitude of the delay introduced by  $^{22}\text{Ne}$  sedimentation was underestimated by a factor of  $\sim 2$ . We also perform a preliminary study of the impact of  $^{22}\text{Ne}$  sedimentation on the white dwarf luminosity function. Finally, we hypothesize on the possibility of detecting the sedimentation of  $^{22}\text{Ne}$  using pulsating white dwarfs in the appropriate effective temperature range with accurately determined rates of change of the observed periods.

*Subject headings:* dense matter — diffusion — stars: abundances — stars: evolution — stars: interiors — white dwarfs

### 1. INTRODUCTION

White dwarf stars are the final evolutionary stage for the vast majority of stars and hence play a key role in our quest for understanding the structure and history of our Galaxy. Standard stellar evolution theory predicts that most white dwarfs are the descendants of post-asymptotic giant branch stars of low and intermediate masses that reach the hot white dwarf stage with hydrogen-rich surface layers. The basic inner structure expected in a typical white dwarf consists of a degenerate core mostly composed of a mixture of carbon and oxygen (the ashes of core helium burning resulting from the evolution of the progenitor) plus some impurities resulting from the original metal content of the progenitor star. The most important of these impurities is  $^{22}\text{Ne}$ , which results from helium burning on  $^{14}\text{N}$ , built up during the CNO cycle of hydrogen burning, and reaches an abundance by mass of  $X_{\text{Ne}} \approx Z_{\text{CNO}} \approx 0.02$  in Population I stars.

An accurate determination of the rate at which white dwarfs cool down constitutes a fundamental issue and provides an independent and valuable cosmic clock to determine ages of many Galactic populations, including the disk (Winget et al. 1987; García-Berro et al. 1988; Hernanz et al. 1994) and globular and open clusters (Richer et al. 1997; Von Hippel & Gilmore 2000; Hansen

et al. 2002; Von Hippel et al. 2006). Thus, considerable effort has been devoted to observationally determining the luminosity function of field white dwarfs (which also provides a measure of the cooling rate) and to empirically determining the observed white dwarf cooling sequence in stellar clusters. In addition, and from the theoretical point of view, the development of very detailed white dwarf evolutionary models that incorporate a complete description of the main energy sources has also been a priority, since these would allow a meaningful comparison with the increasing wealth of observational data (Fontaine et al. 2001; Salaris et al. 2000; Althaus & Benvenuto 1998).

White dwarf evolution can be basically described as a simple cooling process (Mestel 1952) in which the decrease in the thermal heat content of the ions constitutes the main source of luminosity. The release of both latent heat (Van Horn 1968; Lamb & Van Horn 1975) and gravitational energy due to a change in chemical composition during crystallization (Stevenson 1980; García-Berro et al. 1988; Segretain et al. 1994; Isern et al. 1991, 2000) also considerably affects the cooling of white dwarfs. In particular, compositional separation at crystallization temporarily slows down the cooling. This, in turn, influences the position of the cutoff of the disk white dwarf luminosity function (Hernanz et al. 1994), which is essential in obtaining an independent determination of the age of the Galactic disk.

Another potential source of energy is the minor species rich in neutrons, such as  $^{22}\text{Ne}$ . Indeed, as first noted by Bravo et al. (1992) the two extra neutrons present in the  $^{22}\text{Ne}$  nucleus (relative to

<sup>1</sup> Also at: Institut d'Estudis Espacials de Catalunya, c/ Gran Capità 2-4, 08034 Barcelona, Spain.

<sup>2</sup> Member of the Carrera del Investigador Científico y Tecnológico, CONICET (IALP), Argentina.

$A = 2Z$ ) result in a net downward gravitational force and a slow, diffusive settling of  $^{22}\text{Ne}$  in the liquid regions toward the center of the white dwarf. The role of  $^{22}\text{Ne}$  sedimentation in the energetics of crystallizing white dwarfs was first addressed by Isern et al. (1991). The extent to which the cooling of a white dwarf could be modified by this process was later investigated by Bildsten & Hall (2001) and quantitatively explored by Deloye & Bildsten (2002). Deloye & Bildsten (2002) concluded that, depending on the underlying uncertainties in the physics of the interdiffusion coefficients,  $^{22}\text{Ne}$  sedimentation could release sufficient energy to affect appreciably the cooling of massive white dwarfs, making them appear bright for very long periods of time, of the order of  $10^9$  yr. Deloye & Bildsten (2002) predicted that the possible impact of  $^{22}\text{Ne}$  sedimentation on white dwarf cooling could be seen in metal-rich clusters. In fact, white dwarfs resulting from progenitors formed in metal-rich systems are expected to have larger abundances of  $^{22}\text{Ne}$  in their cores, and the delay in the cooling history of white dwarfs resulting from  $^{22}\text{Ne}$  diffusion would be largely amplified in these clusters.

The recent detection of a markedly bright white dwarf population in the old open cluster NGC 6791 (Bedin et al. 2005) is certainly promising in this regard. Indeed, the significant super-solar metallicity characterizing NGC 6791 (about  $[\text{Fe}/\text{H}] \sim +0.4$ ) turns this cluster into a unique target to test the predictions of Deloye & Bildsten (2002), who claim that the effects of sedimentation would be largest in this cluster. Although the anomalously bright white dwarf luminosity function observed in NGC 6791 could be reflecting the presence of a large population of massive white dwarfs with helium cores instead of carbon-oxygen cores, as suggested by Hansen (2005),  $^{22}\text{Ne}$  diffusion constitutes a viable explanation for the morphology of the observed white dwarf luminosity function that cannot be discarded (Kalirai et al. 2007).

In view of these considerations, a full and consistent treatment of white dwarf evolution is required to ascertain the validity of the predictions of Deloye & Bildsten (2002) about the role of  $^{22}\text{Ne}$  diffusion in cooling white dwarfs, since their findings were obtained using a simplified treatment of white dwarf evolution. In particular, although Deloye & Bildsten (2002) carried out a full numerical calculation of the diffusion process, the white dwarf cooling sequences were computed using a series of static white dwarf mechanical configurations in which the thermal evolution of the white dwarf was decoupled, and moreover, the authors did not mention whether or not the mechanical structure of the white dwarf was recomputed self-consistently at each time step. Another crucial point is that the white dwarf models of Deloye & Bildsten (2002) were constructed using a fully degenerate equation of state everywhere (with no inclusion of ion contributions in the structure calculation). This assumption is valid for the white dwarf interior, where the degeneracy is high, but not for the outer nondegenerate parts of the star. In addition, the treatment of Deloye & Bildsten (2002) required as an additional input a relationship between the luminosity of the white dwarf and the temperature of the core (for which they adopted the results of Althaus & Benvenuto 1998), which, additionally, was assumed to be isothermal. As a result, the heat sources and sinks could only be evaluated globally and not locally as we do here. Consequently, these authors could not obtain absolute ages but, rather, relative delays with respect to the absolute ages derived by Althaus & Benvenuto (1998). The aim of the present work is precisely to fill this gap. Specifically, we present a set of full evolutionary and self-consistent white dwarf cooling sequences, which include an accurate treatment of time-dependent  $^{22}\text{Ne}$  diffusion and the physical state of the white dwarf interior.

Special emphasis is given to the treatment of the luminosity equation, particularly regarding the contribution to the energy balance of the terms resulting from changes in the profiles of chemical abundances. Calculations are followed down to very low surface luminosities. The plan of the paper is as follows. Section 2 contains details about the input physics of our white dwarf evolutionary code and the main aspects of the diffusion treatment. In § 3 we present our results. Finally, § 4 is devoted to discussing and summarizing our findings.

## 2. INPUT OF THE MODELS AND EVOLUTIONARY SEQUENCES

### 2.1. General Description of the Code

In this work we have computed the evolution of white dwarfs self-consistently, taking into account the changes in the abundance profiles induced by the gravitational settling of  $^{22}\text{Ne}$ . That is, we have solved the full set of equations describing the structure and evolution of white dwarfs with the luminosity equation appropriately modified to account for the energy released by the changes in the core abundances as a consequence of  $^{22}\text{Ne}$  sedimentation. Consequently, this study constitutes a notable improvement with respect to the approach adopted by Deloye & Bildsten (2002) to compute the white dwarf cooling sequences, where all energy sources were treated as global quantities.

The evolutionary code employed in this study is the one we used in our study of the evolution of massive white dwarf stars (Althaus et al. 2007), modified to incorporate the effects of  $^{22}\text{Ne}$  sedimentation in the interior of white dwarfs. In particular, the equation of state for the high-density regime is very detailed; it is described in Segretain et al. (1994). It accounts for all the important contributions for both the liquid and solid phases. The release of latent heat on crystallization, which is assumed to occur when the ion coupling constant reaches  $\Gamma = 180$  (Stringfellow et al. 1990; Chabrier 1993), and neutrino emission rates have been included following Althaus et al. (2007). Radiative opacities are those from OPAL (Iglesias & Rogers 1996) complemented at low temperatures by the Alexander & Ferguson (1994) molecular opacities. Chemical redistribution due to phase separation on crystallization has not been considered in this work. Particular attention is given to the treatment of the very outer layers of our models at advanced stages of evolution. This is crucial in determining absolute ages. In particular, compression of these layers constitutes the main energy source of the white dwarf when it enters the Debye regime. In the present calculations, the internal solutions of the Henyey iteration have been considered up to a fitting mass fraction of  $\approx 10^{-14} M_r$ .

The initial white dwarf configuration from which we started our calculations of the cooling sequences corresponds to hot white dwarf structures that were obtained following the artificial evolutionary procedure described in Althaus et al. (2005). Because the impact of  $^{22}\text{Ne}$  diffusion on the cooling times is irrelevant for the hot white dwarf regime, the precise selection of the initial conditions bears virtually no relevance for the purposes of the present work. We compute the evolution of white dwarf models with stellar masses of 0.6 and 1.06  $M_{\odot}$ . More massive white dwarfs are expected to have cores composed mainly of oxygen and neon, the result of carbon burning in semidegenerate conditions in the progenitor star (Ritossa et al. 1996; García-Berro et al. 1997). The core chemical profile of our models consists of a predominant chemical element (either carbon or oxygen) plus  $^{22}\text{Ne}$  with an initially flat abundance throughout the core. The abundance of  $^{22}\text{Ne}$  results from helium burning on  $^{14}\text{N}$  via

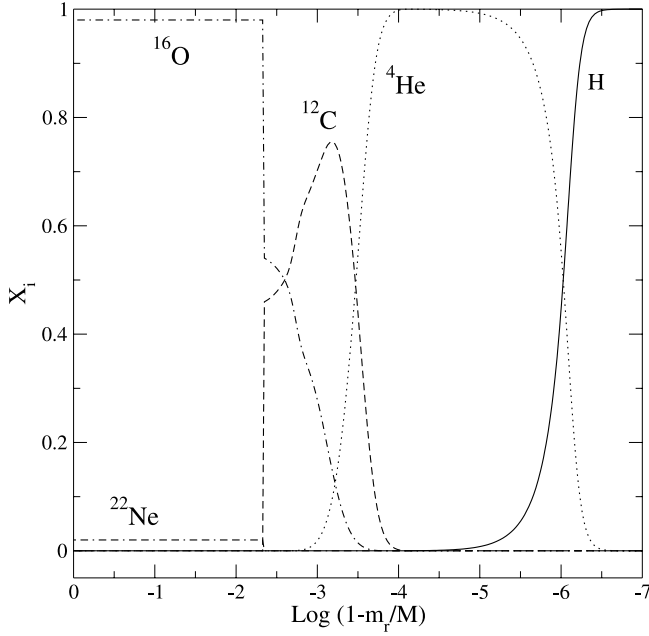


FIG. 1.—Initial chemical abundance distribution for our  $1.06 M_{\odot}$  oxygen-rich core white dwarf.

the reactions  $^{14}\text{N}(\alpha, \gamma)^{18}\text{F}(\beta^+)^{18}\text{O}(\alpha, \gamma)^{22}\text{Ne}$ . In this work, we explore the evolution of white dwarfs resulting from Population I star progenitors, i.e., characterized by  $X_{\text{Ne}} \approx Z_{\text{CNO}} \approx 0.02$ . Although the theory of stellar evolution predicts the core of most white dwarfs to be composed essentially of a mixture of carbon and oxygen, we assume either carbon- or oxygen-dominated cores to be consistent with the one-component plasma underlying assumption in the derivation of the diffusion coefficient. The outer layer chemical stratification of all of our models consists of a pure hydrogen envelope of  $10^{-6} M_{\star}$  (plus a small inner tail) overlying a helium-dominated shell and, below that, a buffer rich in carbon and oxygen. The initial chemical stratification corresponding to an oxygen-rich  $1.06 M_{\odot}$  white dwarf is displayed in Figure 1. The shape of the outer layer chemical profile is given by element diffusion at low luminosities. Nevertheless, diffusion occurring in the outer layers was switched off in the present calculations. The evolutionary stages computed cover the luminosity range from  $\log(L/L_{\odot}) \approx 0$  down to  $-5.3$ .

For a proper treatment of white dwarf evolution in a self-consistent way with the changes in the core chemical composition induced by  $^{22}\text{Ne}$  sedimentation, the standard luminosity equation for evolving white dwarfs (thermonuclear reactions are neglected),

$$\frac{\partial L_r}{\partial M_r} = -\epsilon_{\nu} - C_P \dot{T} + \frac{\delta}{\rho} \dot{P}, \quad (1)$$

has to be appropriately modified (see Isern et al. 1997; Kippenhahn et al. 1965). In equation (1),  $\epsilon_{\nu}$  denotes the energy per unit mass per second due to neutrino losses and the other quantities have their usual meaning (Kippenhahn & Weigert 1990). To this end, we write the energy equation in terms of changes in the internal energy per gram ( $u$ ) and density ( $\rho$ ),

$$\frac{\partial L_r}{\partial M_r} = -\epsilon_{\nu} - \dot{u} + \frac{P}{\rho^2} \dot{\rho}, \quad (2)$$

and we assume the white dwarf interior to be made of two chemical elements with abundance by mass  $X_1$  and  $X_2$  ( $X_1 + X_2 = 1$ ), where  $X_1$  refers to the  $^{22}\text{Ne}$  abundance. Now,

$$\dot{u} = \left( \frac{\partial u}{\partial \rho} \right)_{T, X_1} \dot{\rho} + \left( \frac{\partial u}{\partial T} \right)_{\rho, X_1} \dot{T} + \left( \frac{\partial u}{\partial X_1} \right)_{\rho, T} \dot{X}_1, \quad (3)$$

and with the help of the thermodynamic relation

$$\left( \frac{\partial u}{\partial \rho} \right)_{T, X_1} = \frac{P}{\rho^2} - \frac{T}{\rho^2} \left( \frac{\partial P}{\partial T} \right)_{\rho, X_1}, \quad (4)$$

equation (2) can be rewritten as

$$\frac{\partial L_r}{\partial M_r} = -\epsilon_{\nu} + \frac{T}{\rho^2} \left( \frac{\partial P}{\partial T} \right)_{\rho, X_1} \dot{\rho} - C_P \dot{T} - \left( \frac{\partial u}{\partial X_1} \right)_{\rho, T} \dot{X}_1. \quad (5)$$

Finally, by taking into account that fact that  $\rho = \rho(P, T, X_1)$  and the definitions

$$\delta = - \left( \frac{\partial \ln \rho}{\partial \ln T} \right)_{P, X_1},$$

$$\alpha = \left( \frac{\partial \ln \rho}{\partial \ln P} \right)_{T, X_1}.$$

equation (5) can be written as

$$\frac{\partial L_r}{\partial M_r} = -\epsilon_{\nu} - C_P \dot{T} + \frac{\delta}{\rho} \dot{P} - A \dot{X}_1, \quad (6)$$

where  $A$  is given by

$$A = \left( \frac{\partial u}{\partial X_1} \right)_{\rho, T} - \frac{P\delta}{\alpha\rho^2} \left( \frac{\partial \rho}{\partial X_1} \right)_{P, T}, \quad (7)$$

or alternatively

$$A = \left( \frac{\partial u}{\partial X_1} \right)_{\rho, T} + \frac{\delta}{\rho} \left( \frac{\partial P}{\partial X_1} \right)_{\rho, T}. \quad (8)$$

The second and third terms of equation (6) are the well-known contributions of the heat capacity and pressure changes to the local luminosity of the star. The fourth term represents the energy released by chemical abundance changes. Although this term is usually small for most stages of stellar evolution (as compared to the release of nuclear energy; Kippenhahn et al. 1965), it will play, as will be clear below, a major role in the cooling of white dwarfs with diffusively evolving core chemical compositions. For neutron-rich species, such as in the problem of  $^{22}\text{Ne}$  diffusion in the core of white dwarfs, the derivative  $(\partial u / \partial X_1)_{\rho, T}$  is dominated by the electronic contributions. Thus,  $A$  becomes negative and the last term in equation (6) will be a source (sink) of energy in those regions where diffusion leads to an increase (decrease) in the  $^{22}\text{Ne}$  local abundance. In simpler terms, an increase (decrease) in the  $^{22}\text{Ne}$  abundance, or in the molecular weight per electron  $\mu_e$ , will force the electron gas to release (absorb) energy. Finally, in equation (6) we have included a term that represents the contribution of latent heat of crystallization ( $\approx k_B T$  per ion, where  $k_B$  is the Boltzmann constant).

## 2.2. Treatment of Diffusion

The evolution of the core chemical abundance distribution caused by  $^{22}\text{Ne}$  diffusion has been fully accounted for. In presence of partial gradients, gravitational and electric forces, the diffusion velocities satisfy the set of equations (Burgers 1969)

$$\frac{dp_i}{dr} - \frac{\rho_i}{\rho} \frac{d\rho}{dr} - n_i Z_i e E = \sum_{j \neq i}^N K_{ij} (w_j - w_i). \quad (9)$$

Here  $p_i$ ,  $\rho_i$ ,  $n_i$ ,  $Z_i$ , and  $w_i$  are, respectively, the partial pressure, mass density, number density, charge, and diffusion velocity for species  $i$ , and  $N$  is the number of ionic species plus electron. The unknown variables are  $w_i$  and the electric field  $E$ . The resistance coefficients are denoted by  $K_{ij}$ . For the white dwarf core we are mainly interested in the gravitational settling, thus we drop off the first term in equation (9). The core of our white dwarf models consists of a predominant ion species, either  $^{16}\text{O}$  or  $^{12}\text{C}$  plus  $^{22}\text{Ne}$  (these two species are denoted by the subscripts 2 and 1, respectively). We assume the electron to have zero mass. Since  $\rho_i = A_i n_i m_p$ , equation (9) can be written in the form

$$A_1 n_1 m_p g - n_1 Z_1 e E = K_{12} (\omega_2 - \omega_1), \quad (10)$$

$$A_2 n_2 m_p g - n_2 Z_2 e E = K_{21} (\omega_1 - \omega_2), \quad (11)$$

$$A_1 n_1 \omega_1 + A_2 n_2 \omega_2 = 0. \quad (12)$$

Here  $g$  is the local gravitational acceleration,  $m_p$  is the proton mass, and  $A_i$  is the atomic mass number. The last equation is the condition for no net mass flow relative to the center of mass. From the last set of equations we find that the diffusion velocities (with the effect of the induced electric field considered) are

$$w_1 = \left( \frac{A_2}{Z_2} - \frac{A_1}{Z_1} \right) \frac{m_p g D}{k_B T} \frac{(n_1 + n_2)}{n_1 n_2 f}, \quad (13)$$

$$w_2 = - \frac{A_1 n_1}{A_2 n_2} w_1, \quad (14)$$

where  $f = (1 + A_1 n_1 / A_2 n_2) (n_1 Z_1 + n_2 Z_2) / n_1 Z_1 n_2 Z_2$ , and we have introduced the diffusion coefficient  $D$  as

$$D = \frac{k_B T n_1 n_2}{(n_1 + n_2) K_{12}}. \quad (15)$$

For  $^{22}\text{Ne}$ ,  $A_1 = 22$  and  $Z_1 = 10$ , while for either  $^{16}\text{O}$  or  $^{12}\text{C}$ ,  $A_2/Z_2 = 2$ . Thus, we arrive at

$$w_1 = - \frac{1}{5} \frac{m_p g D}{k_B T} \frac{(n_1 + n_2)}{n_1 n_2 f}, \quad (16)$$

$$w_2 = \frac{1}{5} \frac{m_p g D}{k_B T} \frac{A_1}{A_2} \frac{(n_1 + n_2)}{n_2^2 f}. \quad (17)$$

The negative sign for the  $^{22}\text{Ne}$  velocity reflects the fact that this ion settles toward the center of the white dwarf. This is expected because of the two excess neutrons of the  $^{22}\text{Ne}$  nucleus (in comparison with  $A = 2Z$ ). Note that if  $^{22}\text{Ne}$  is assumed to be a trace element ( $n_1 \approx 0$ ) then  $(n_1 + n_2) / n_1 n_2 f \approx Z_1$  and we re-

cover the diffusion velocity of Bildsten & Hall (2001) and Deloye & Bildsten (2002), namely,  $w_{\text{Ne}} = -2m_p g D / k_B T$ .

For the diffusion coefficient  $D$  we follow the treatment adopted by Deloye & Bildsten (2002) for the self-diffusion coefficient in one-component plasmas. In the liquid interior  $D$  becomes (in units of square centimeters per second)

$$D_s = \frac{7.3 \times 10^{-7} T}{\rho^{1/2} Z_2 \Gamma^{1/3}}, \quad (18)$$

where  $\Gamma$  is the Coulomb coupling constant. For the regions of the white dwarf that have crystallized, diffusion is expected to be no longer efficient due to the abrupt increase in viscosity expected in the solid phase. Thus, we set  $D = 0$  in the crystallized regions. To avoid numerical difficulties, the value of  $D$  is reduced from  $D_s$  to 0 in the solid phase over a small range of  $\Gamma$ -values. To assess the consequences of possible uncertainties in the values of  $D$ , we have also performed evolutionary calculations for the case  $D = 5D_s$ . In addition, we have explored the less likely situation in which white dwarfs experience a glassy transition at high  $\Gamma$ -values instead of crystallizing. In a glassy state, diffusion is expected to continue. For this regime, viscosity increases considerably with the consequent reduction in the diffusion coefficient. If we also follow Deloye & Bildsten (2002), the diffusion coefficient in the glassy state is reduced as  $D_{\text{glass}} = D_s / f^*$  with  $f^* = 1 + 5.4 \times 10^{-7} \Gamma^{2.3666} + 2.16 \times 10^{-27} \Gamma^{9.3666}$ .

The evolution of the chemical abundance distribution in the core of our white dwarf models caused by diffusion is described in terms of a time-dependent, finite-difference scheme that solves elemental continuity equations for the number densities  $n_i$ . The equation governing the evolution of the number density of species  $i$  in the space variable  $r$  is

$$\frac{\partial n_i}{\partial t} = \frac{1}{r^2} \frac{\partial}{\partial r} \left( r^2 D \frac{\partial n_i}{\partial r} - r^2 \omega_i n_i \right), \quad (19)$$

supplemented with appropriate boundary conditions. Here the diffusive flux caused by ion density gradients and the drifting flux due to gravitational settling are considered. To solve this equation, we follow the method described in Iben & MacDonald (1985). In particular, we discretize equation (19) as

$$n_{i,k} - n_{i,k}^0 = \frac{\Delta t}{\Delta V_k} \left[ - \left( r_{k+1/2}^2 \omega_{i,k+1/2}^0 \frac{n_{i,k} + n_{i,k+1}}{2} - r_{k-1/2}^2 \omega_{i,k-1/2}^0 \frac{n_{i,k} + n_{i,k-1}}{2} \right) + r_{k+1/2}^2 D_{k+1/2}^0 \frac{n_{i,k+1} - n_{i,k}}{\Delta r_{k+1/2}} - r_{k-1/2}^2 D_{k-1/2}^0 \frac{n_{i,k} - n_{i,k-1}}{\Delta r_{k-1/2}} \right], \quad (20)$$

where the superscript 0 means that quantities are to be evaluated at the beginning of the time step  $\Delta t$  and the subscript  $k$  refers to the spatial index;  $\Delta V_k = (r_{k+1/2}^3 - r_{k-1/2}^3) / 3$ , and  $r_{k+1/2}^3 = (r_k^3 + r_{k+1}^3) / 2$ . Note that  $\omega_i$  and  $D$  are also averaged between adjacent grid points. Equation (20) is linear in the unknowns  $n_i$ . We follow the evolution of two chemical species in the core of the white dwarf: either  $^{12}\text{C}$  or  $^{16}\text{O}$ , and  $^{22}\text{Ne}$ . In order to compute self-consistently the dependence of the structure and evolution of our white dwarf models on the varying abundances, the set of

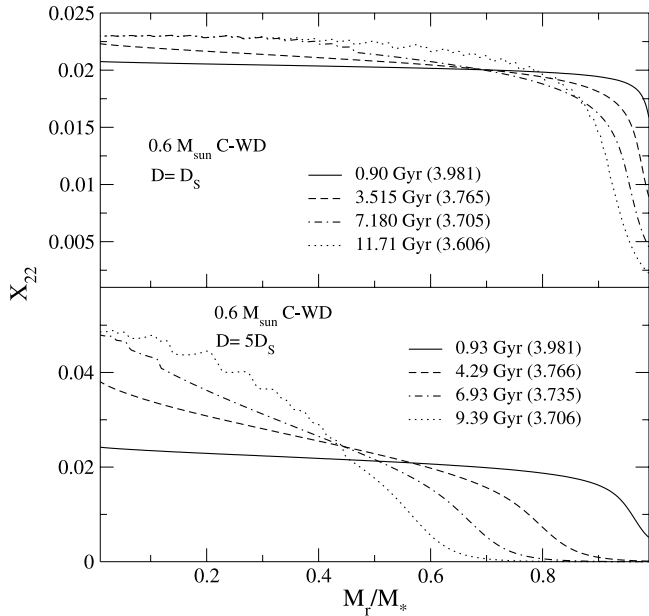


FIG. 2.—Diffusively evolving internal  $^{22}\text{Ne}$  profiles for the  $0.6 M_{\odot}$  carbon-rich white dwarf sequence in terms of the mass fraction at selected evolutionary stages. The ages of the models are indicated in the figure. The numbers in parentheses are the values of  $\log T_{\text{eff}}$  for the corresponding models. The top and bottom panels display the situation for the case in which the diffusion coefficient is set to  $D = D_s$  and  $5D_s$ , respectively.

equations describing diffusion has been coupled to the evolutionary code.

### 3. RESULTS

We begin by examining Figure 2, which displays the diffusively evolving  $^{22}\text{Ne}$  profile in the core of the  $0.6 M_{\odot}$  carbon-rich white dwarf sequence as a function of the mass fraction. The situation at four selected stages of evolution is depicted. Clearly, diffusion appreciably modifies the  $^{22}\text{Ne}$  profile but only after a long enough time has elapsed, causing a strong depletion of its abundance in the outer region of the core, where the diffusion timescale is comparable to the characteristic cooling time of the white dwarf. This is more apparent in the case of very efficient diffusion, as illustrated in the bottom panel of Figure 2, which shows the evolving profiles when  $D = 5D_s$  is adopted. In this case, by the time the white dwarf has started the crystallization process (at  $\log T_{\text{eff}} = 3.753$ ) diffusion has completely depleted  $^{22}\text{Ne}$  in the outermost region (20% by mass) of the white dwarf, and has markedly enhanced the abundance of  $^{22}\text{Ne}$  in the central regions of the star. As crystallization proceeds, it leaves recognizable imprints in the inner  $^{22}\text{Ne}$  profile. This is because diffusion is not operative in the crystallized region, thus forcing  $^{22}\text{Ne}$  to accumulate at the crystallization front. As the crystallization front moves outward, an apparently irregular profile is left behind, as clearly seen in Figure 2. The apparent wave in the  $^{22}\text{Ne}$  abundance in the crystallized core is a numerical artifact (see the discussion about this issue in Deloye & Bildsten 2002). This irregular profile, which arises from the use of finite time steps in the evolutionary calculation and because diffusion is switched off at the liquid-solid boundary that occurs over a finite range of  $\Gamma$ -values, bears no relevance for the calculation of the cooling ages of the white dwarfs.

The rate at which  $^{22}\text{Ne}$  diffuses downward increases markedly with gravity. Thus, we expect a more rapid sedimentation and a faster depletion of  $^{22}\text{Ne}$  in the outer layers of massive white dwarfs.

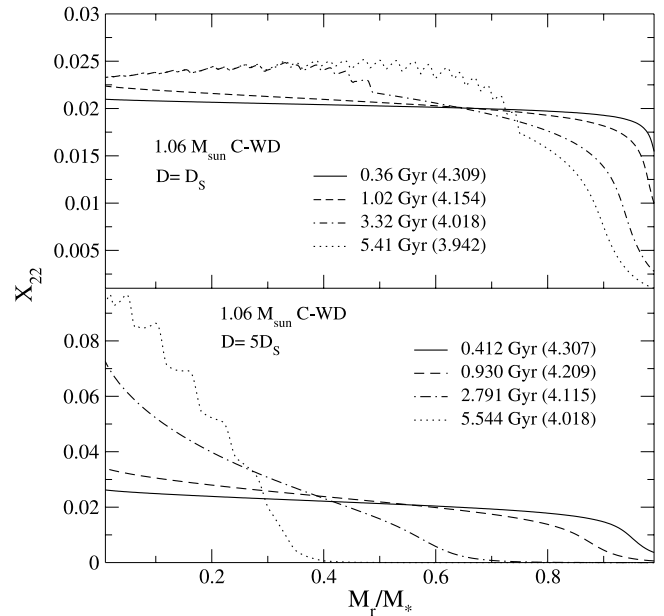


FIG. 3.—Same as Fig. 2, but for the  $1.06 M_{\odot}$  carbon-rich white dwarf models.

This is shown in Figure 3, which illustrates the  $^{22}\text{Ne}$  profile evolution for various  $1.06 M_{\odot}$  carbon-rich white dwarf models. The results for  $D = 5D_s$ , shown in the bottom panel of this figure, are worthy of comment. Indeed, while the white dwarf remains in a liquid state (at effective temperatures  $\log T_{\text{eff}} > 4.12$ ), the  $^{22}\text{Ne}$  abundance distribution will be strongly modified by diffusion during the evolution. Note that by the time the white dwarf begins to crystallize,  $^{22}\text{Ne}$  has diffused so deep into the core that no trace of this element is found in layers even as deep as  $0.4 M_{\odot}$  below the stellar surface. Note also the marked accumulation of  $^{22}\text{Ne}$  toward the central regions. Shortly after, at  $\log T_{\text{eff}} \approx 4.02$ , about half the white dwarf mass is crystallized and the  $^{22}\text{Ne}$  distribution will remain frozen with further cooling. Because massive white dwarfs crystallize earlier than less massive ones,  $^{22}\text{Ne}$  diffusion will end at much higher effective temperatures when compared with less massive white dwarfs. This is a critical issue regarding the cooling ages of massive white dwarfs, as will be discussed below.

It is clear from Figures 2 and 3 that diffusion substantially changes the core abundance distribution of  $^{22}\text{Ne}$  in the course of white dwarf evolution. These changes are in good agreement with those reported by Deloye & Bildsten (2002). We thus would expect that the contribution to the local energy budget of the white dwarf stemming from the last term in equation (6) could play a significant role. We show this in Figure 4 for the same  $1.06 M_{\odot}$  carbon-rich stellar models shown in the top panel of Figure 3. Figure 4 clearly illustrates the fact that  $^{22}\text{Ne}$  diffusion constitutes a local source or sink of energy depending on whether the local abundance of  $^{22}\text{Ne}$  increases or decreases. In fact, note that for those regions where diffusion has increased the local abundance of  $^{22}\text{Ne}$ ,  $A\dot{X}_{22} < 0$ . Thus, this term constitutes an energy source in such regions; in fact, the increase in the molecular weight  $\mu_e$  forces the electron gas to release energy. In the outermost part of the core, however, where  $^{22}\text{Ne}$  depletion occurs,  $A\dot{X}_{22} > 0$ , thus implying a sink of energy in those regions. To compare with the main standard contribution to  $L_r$ , we include in Figure 4 the run of  $C_p \dot{T}$  (the second term in eq. [6]) as a thin solid line. We do this for the model with  $\log T_{\text{eff}} = 4.154$ , which corresponds to the model shown with dashed line. We have chosen this model because it corresponds to an evolutionary stage just

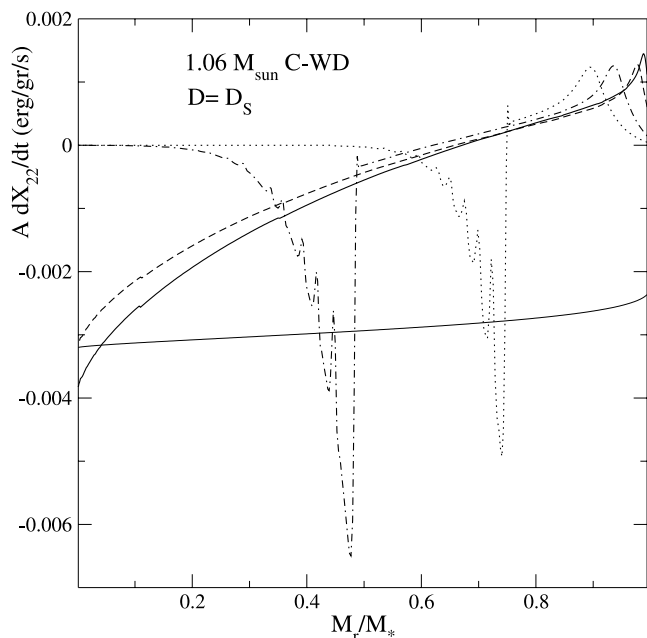


FIG. 4.—Local energy contribution resulting from changes in the  $^{22}\text{Ne}$  abundance (the term  $-A\dot{X}_1$  in eq. [6]) for the same  $1.06 M_{\odot}$  carbon-rich white dwarf models shown in the top panel of Fig. 3. The thin line denotes the heat capacity contribution for the model with  $\log T_{\text{eff}} = 4.154$ . Note that in the outer regions of the core,  $^{22}\text{Ne}$  diffusion constitutes an energy sink ( $A\dot{X}_1 > 0$ ).

before the onset of crystallization. For this model, the energy contribution from  $^{22}\text{Ne}$  diffusion near the center of the white dwarf is similar to the heat capacity contribution of about  $0.003 \text{ erg g}^{-1} \text{ s}^{-1}$ . Finally, the dot-dashed and dotted curves correspond, respectively, to models for which 50% and 75% of their mass has already crystallized. The  $^{22}\text{Ne}$  accumulation at the crystallization front leads to a large local energy contribution, restricted to a very narrow mass range. Because diffusion stops in the crystallized interior, the  $^{22}\text{Ne}$  profile remains frozen there, and the term  $A\dot{X}_1$  vanishes. This fact limits the extent to which  $^{22}\text{Ne}$  diffusion constitutes an energy source for the star.

From the above discussion, it is expected that the  $^{22}\text{Ne}$  profile evolution affects the fractional luminosity of the white dwarfs. This is exemplified in the top panel of Figure 5, which shows the fractional luminosity  $L_r$  in terms of the fractional mass  $M_r$  for the same  $1.06 M_{\odot}$  carbon-rich white dwarf stellar models shown in Figure 4. The bottom panel displays the behavior for the case in which  $^{22}\text{Ne}$  diffusion is not considered. In both cases, the imprint of the latent heat release on crystallization is apparent in the models with  $\log T_{\text{eff}} = 4.018$  and  $3.942$ . There is clearly an important contribution of the  $^{22}\text{Ne}$  diffusion to the luminosity budget of massive white dwarfs. This contribution is notably enhanced when a larger diffusion coefficient is considered, as becomes clear from Figure 6, which shows the same quantity for the case in which  $D = 5D_S$  is adopted. The models plotted in Figure 6 are the same as those shown in the bottom panel of Figure 3. Note that the fractional luminosity profile is indeed strongly modified in this case. Particularly relevant is the model with  $\log T_{\text{eff}} = 4.115$  (dot-dashed line), which already has a small crystalline core. In fact, its internal luminosity at  $M_r \approx 0.3M_*$  is about twice the luminosity emerging from the surface. Note also the strong decrease in the fractional luminosity in the outer layers of this model, which results from the depletion of  $^{22}\text{Ne}$  in these layers (see Fig. 3, *bottom*) with the consequent energy absorption.

To get a deeper insight of the importance of  $^{22}\text{Ne}$  diffusion into the global energetics during the whole white dwarf evolution,

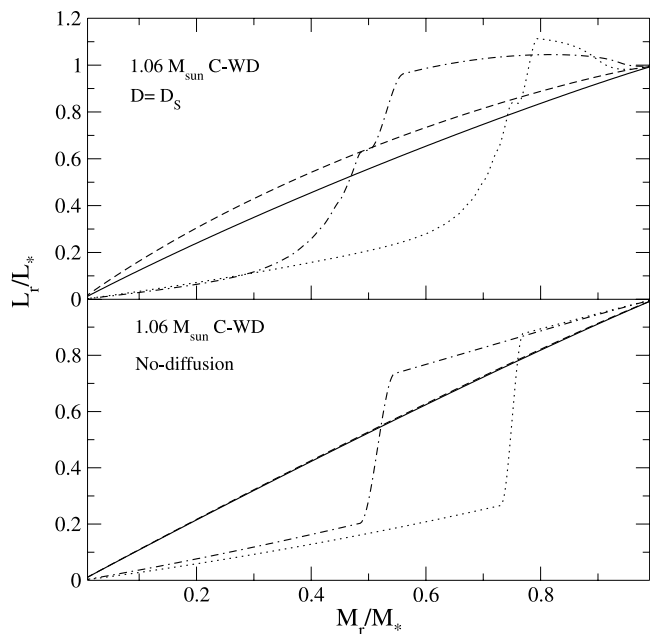


FIG. 5.—*Top*: Fractional luminosity in terms of the fractional mass for the same  $1.06 M_{\odot}$  carbon-rich white dwarf models shown in the top panel of Fig. 3. *Bottom*: Same quantity for the case in which  $^{22}\text{Ne}$  diffusion is not considered.

we show in Figure 7 the resulting luminosity contribution obtained by integrating at each effective temperature the term  $-A\dot{X}_1$  in equation (6) throughout all the star. The result (expressed in solar units) is shown in terms of the white dwarf effective temperature for the  $1.06 M_{\odot}$  cooling sequences. The top panel corresponds to white dwarf sequences with carbon-rich cores. To highlight the role of the core chemical composition, the bottom panel shows the sequences with oxygen-rich cores. Several aspects deserve comments. To begin with, note that because of the high photon luminosity of the star, the luminosity contribution from  $^{22}\text{Ne}$  sedimentation is of a very minor importance during the hot white dwarf stages. It is only after the onset of core

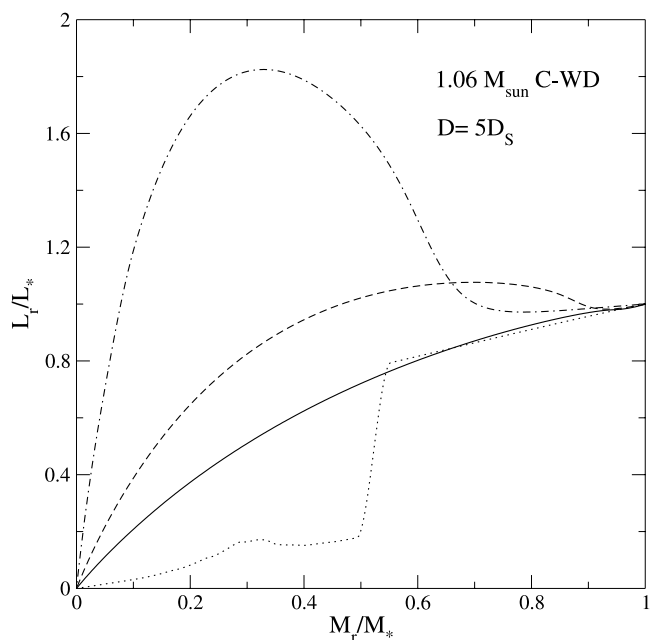


FIG. 6.—Fractional luminosity in terms of the fractional mass for the same  $1.06 M_{\odot}$  carbon-rich white dwarf models shown in the bottom panel of Fig. 3, for the case in which we adopt  $D = 5D_S$ .

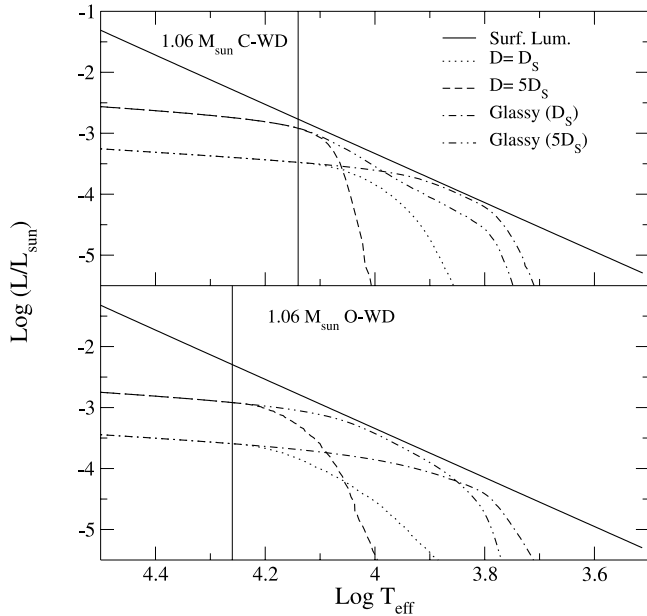


FIG. 7.—Luminosity contribution in solar units resulting from  $^{22}\text{Ne}$  diffusion in terms of the white dwarf effective temperature for  $1.06 M_{\odot}$  sequences with carbon- and oxygen-rich cores (*top and bottom, respectively*). Dotted and dashed lines are the results for  $D = D_s$  and  $5D_s$ , respectively, while the remaining curves correspond to the cases when models enter a glassy state. For the latter situation, we show results for  $D = D_{\text{glass}}$  and  $5D_{\text{glass}}$ . The solid line displays the surface luminosity. The vertical line marks the approximate value of the effective temperature for the onset of core crystallization.

crystallization that this energy source contributes appreciably to the star luminosity. This is particularly true for the case of carbon-rich models, which crystallize at lower surface luminosities than their oxygen-rich counterparts. Because of the rapid crystallization of the core,  $^{22}\text{Ne}$  diffusion luminosity declines steeply with further cooling. This decline occurs earlier in the case  $D = 5D_s$  because of the rapid depletion of  $^{22}\text{Ne}$  in the outer layers in this case (see Fig. 3). A similar behavior was reported by Deloye & Bildsten (2002). As illustrated in the bottom panel of Figure 7, the impact of  $^{22}\text{Ne}$  settling in the energetics of white dwarfs with oxygen-rich cores is less relevant than in the case of carbon-rich ones. Finally, for both core compositions, we compute the  $^{22}\text{Ne}$  settling luminosity for the case in which the white dwarf is assumed to experience a transition to a glassy state at high  $\Gamma$ -values instead of crystallizing. We show this for the cases  $D = D_{\text{glass}}$  and  $5D_{\text{glass}}$  (*dot-dashed and double-dot-dashed lines, respectively*). Because diffusion is operative in a glassy state,  $^{22}\text{Ne}$  settling luminosity obviously persists in more advanced stages of the evolution, providing the bulk of star luminosity at small effective temperatures. This is particularly true for the case  $D = 5D_{\text{glass}}$ . However, at very low effective temperatures, the viscosity increase in the glassy state prevents diffusion from occurring, and the luminosity contribution eventually declines.

For low-mass white dwarfs, the impact of  $^{22}\text{Ne}$  settling is expectedly much less noticeable, albeit not negligible, particularly in the case of carbon-rich white dwarfs and efficient diffusion (see Fig. 8). Note that because  $^{22}\text{Ne}$  sedimentation is a slower process in low-mass white dwarfs, it will take long for  $^{22}\text{Ne}$  settling to contribute to the energy budget of the star. Since less massive white dwarfs crystallize at much lower effective temperatures than massive ones, this contribution will play some role at the very late stages of evolution. It is worth noting that the qualitative behavior of the evolution of the global energetics of our full sequences resembles that reported by Deloye & Bildsten

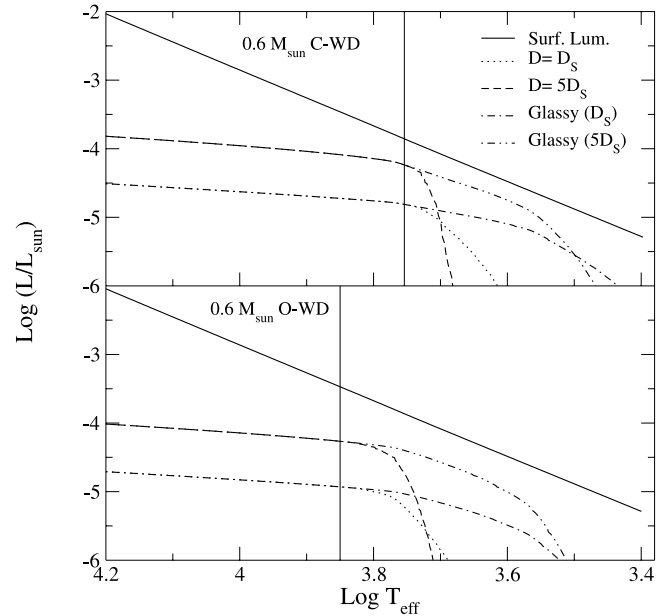


FIG. 8.—Same as Fig. 7, but for the  $0.6 M_{\odot}$  white dwarf sequences.

(2002). In part, this is expected since, as noted by Deloye & Bildsten (2002), the diffusion timescale in the white dwarf core is much longer than the time on which energy is transferred through the core. We expect then a similar behavior between both sets of calculations, as discussed below.

The impact of  $^{22}\text{Ne}$  sedimentation in the white dwarf cooling ages is seen in Figures 9 and 10 for the  $1.06$  and  $0.6 M_{\odot}$  white dwarf cooling sequences, respectively. Here the white dwarf surface luminosity is shown as a function of the age. The solid line corresponds to the standard case when  $^{22}\text{Ne}$  diffusion is not considered. The top and bottom panels of each of these figures are for carbon- and oxygen-rich cores, respectively. Clearly,  $^{22}\text{Ne}$  diffusion profoundly influences the cooling times, particularly those of massive white dwarfs. This influence becomes more dramatic in the case of efficient diffusion—that is, the case in which  $D = 5D_s$  is adopted—which corresponds to the dashed curves. The star will spend a long time getting rid of the energy released by the diffusion-induced abundance changes, with the consequent marked lengthening of evolutionary times persisting until low luminosities. From the discussion in the preceding paragraph, it is evident that the signatures of  $^{22}\text{Ne}$  diffusion in the white dwarf cooling track start to manifest themselves earlier in more massive white dwarfs, at  $\log(L/L_{\odot}) \approx -2$ . The delay in the cooling times depends not only on the stellar mass, but also markedly on the chemical composition of the core. For instance, for the case  $D = 5D_s$ , the delays introduced in the  $1.06 M_{\odot}$  carbon-rich sequence amount to 2.45 and 3.24 Gyr at  $\log(L/L_{\odot}) \approx -3$  and  $-4$ , respectively, as compared with 0.5 and 0.6 Gyr in the case of the oxygen-rich sequence. In low-mass white dwarfs, appreciable delays in the cooling rates take place but only at low luminosities and for efficient diffusion.

The cooling rate in the case that white dwarfs experience a transition to a glassy state behaves differently since in this case  $^{22}\text{Ne}$  sedimentation continues releasing energy even at very large  $\Gamma$ -values. This distinct behavior can be appreciated in the two cooling curves of the  $1.06 M_{\odot}$  carbon-rich sequences shown as dashed and double-dot-dashed curves, which correspond, respectively, to a sequence that experiences crystallization (with  $D = 5D_s$ ) and to a sequence that undergoes a glassy transition (with  $D = 5D_{\text{glass}}$ ). In fact, the decline in the luminosity contribution

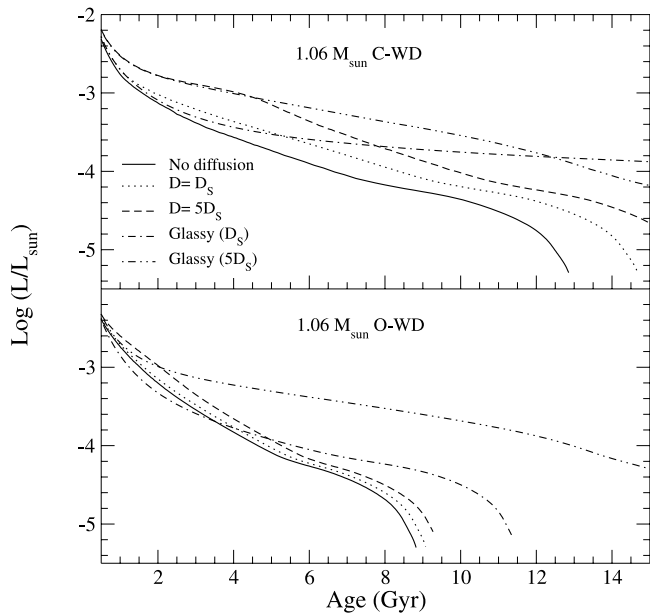


FIG. 9.—Surface luminosity vs. age for the  $1.06 M_{\odot}$  white dwarf sequences with carbon- and oxygen-rich cores (*top and bottom, respectively*). The solid line displays the cooling times for the case in which  $^{22}\text{Ne}$  diffusion is not considered. Dotted and dashed lines display the results for  $D = D_s$  and  $5D_s$ , respectively, while the remaining curves correspond to the cases when models enter a glassy state. For the latter situation, we show results for  $D = D_{\text{glass}}$  and  $5D_{\text{glass}}$ .

from  $^{22}\text{Ne}$  sedimentation due to the presence of the crystalline core (see Fig. 7) translates into a change of slope in the cooling curve with  $D = 5D_s$  at  $\log(L/L_{\odot}) \approx -3$ . By contrast, the cooling rate for glassy white dwarfs remains much smaller. We thus expect substantially larger delays in the cooling ages if a transition to a glassy state actually occurs in nature. In this case, massive white dwarfs would remain bright even at exceedingly large ages. Note that during the crystallization stage, sequences that experience a glassy transition (in the case  $D = D_{\text{glass}}$ ) are younger than sequences without diffusion. This is because the glassy white dwarf does not release latent heat. Because crystal-

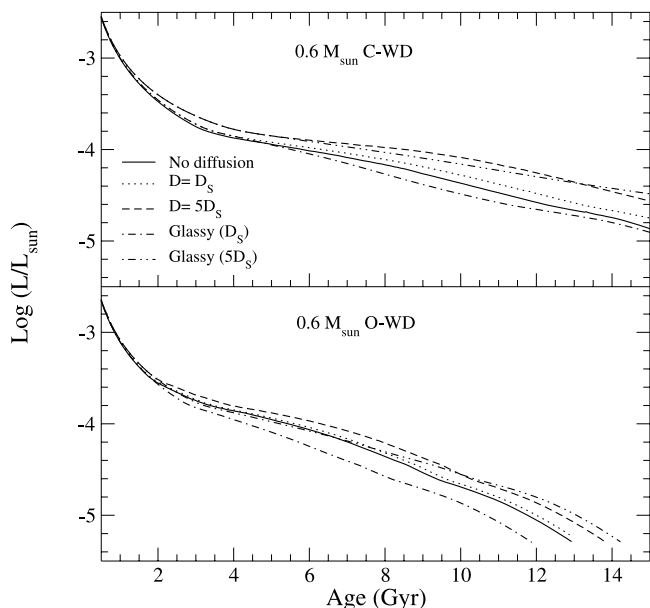


FIG. 10.—Same as Fig. 9, but for the  $0.6 M_{\odot}$  white dwarf sequences.

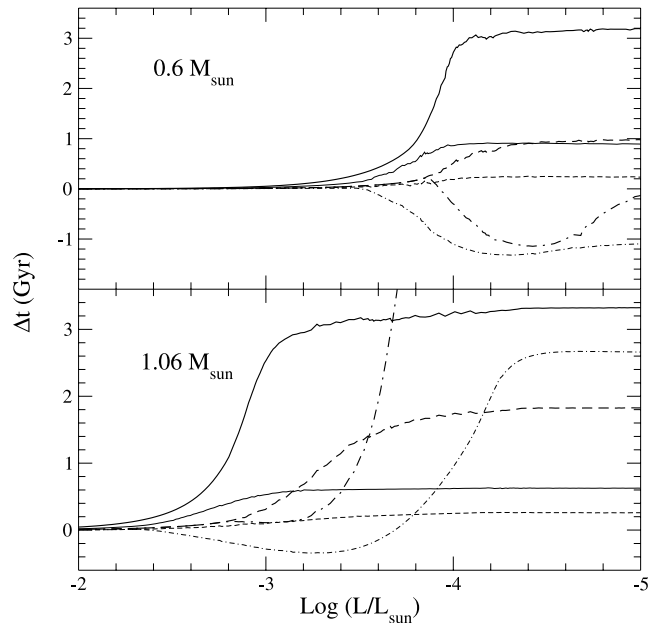


FIG. 11.—Difference in evolutionary times between sequences with various assumptions about diffusion and the sequence in which diffusion is neglected. Solid, dashed, and dot-dashed lines correspond to sequences with  $D = 5D_s$ ,  $D = D_s$ , and the glassy state with  $D = D_{\text{glass}}$ . The thick and thin sets of lines are for the model sequence with carbon-rich and oxygen-rich cores, respectively.

lization is more relevant in less massive white dwarfs, this behavior is more evident in such white dwarfs.

In closing, we note that the more sophisticated and self-consistent treatment of white dwarf evolution with diffusively evolving  $^{22}\text{Ne}$  abundances done in this work yields results that are in qualitative agreement with those of Deloye & Bildsten (2002), which were obtained using a global and much more simplified treatment of white dwarf evolution. However, there are quantitative differences. In the interest of comparison, we show in Figure 11 the age difference between our sequences with  $D = 5D_s$  and  $D_s$  and the sequence in which  $^{22}\text{Ne}$  diffusion is not considered. Results for both carbon-rich and oxygen-rich core compositions are illustrated. This figure can be compared with Figure 10 of Deloye & Bildsten (2002). Although a direct comparison is not easy because Deloye & Bildsten (2002) consider cores composed of a mixture of carbon and oxygen, a close inspection of the two figures reveals that for both stellar masses our calculations predict age differences larger by a factor of  $\sim 2$  when compared with the age differences obtained by Deloye & Bildsten (2002). In fact, we find that the impact of  $^{22}\text{Ne}$  diffusion on the white dwarf cooling ages is substantially more important than originally inferred by Deloye & Bildsten (2002). For the case in which a glassy transition is considered, we find marked differences between both sets of calculations for the low-mass sequence. Indeed, in our calculations, the glassy sequence remains younger than the standard sequence without diffusion throughout the entire evolution (we stress that the glassy sequence does not release latent heat), while in the Deloye & Bildsten (2002) treatment, once the crystallization process is finished, the released energy from  $^{22}\text{Ne}$  diffusion in the glassy sequence yields an age increase.

#### 4. DISCUSSION AND CONCLUSIONS

Motivated by the theoretical proposal that the cooling of white dwarfs could be altered by the sedimentation of  $^{22}\text{Ne}$  in the liquid interior of these stars (Bravo et al. 1992; Bildsten & Hall 2001;



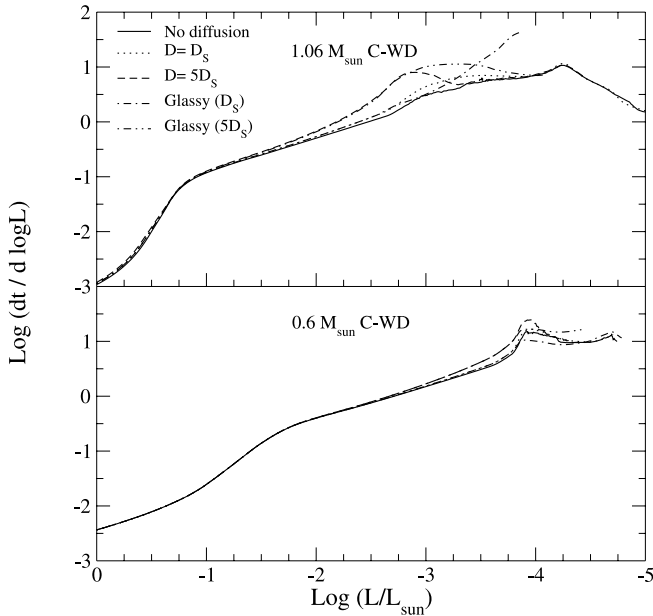


FIG. 12.—Characteristic cooling time  $-dt/d \log(L/L_{\odot})$  for the 1.06 and  $0.6 M_{\odot}$  white dwarf evolutionary sequences with carbon-rich cores as a function of luminosity. The solid line corresponds to the case in which  $^{22}\text{Ne}$  diffusion is not considered. The dotted and dashed lines display the results for  $D = D_s$  and  $5D_s$ , respectively, while the remaining curves correspond to the cases in which the models enter a glassy state. For the latter situation, we show results for  $D = D_{\text{glass}}$  and  $5D_{\text{glass}}$ . Only ages smaller than 14 Gyr have been considered.

Deloye & Bildsten 2002) and the possibility that this could leave imprints in the white dwarf population of metal-rich systems, we have presented in this paper detailed evolutionary calculations to address this issue. These are the first fully self-consistent evolutionary calculations of this effect. We have explored several possibilities. In particular we have thoroughly analyzed two classes of cooling sequences. The first class corresponds to an otherwise typical  $0.6 M_{\odot}$  white dwarf, whereas the second one corresponds to a massive  $1.06 M_{\odot}$  white dwarf. In addition, the effects of the core composition have been addressed by following cooling sequences for carbon cores with a small admixture of  $^{22}\text{Ne}$  and the corresponding ones in which the main constituent of the core was oxygen. The sensitivity of our results to the precise value of the rather uncertain diffusion coefficient has also been explored. Finally, we have also analyzed the effects of assuming that the white dwarf instead of crystallizing at low temperatures experiences a transition to a glassy state. All in all, we have found that the sedimentation of  $^{22}\text{Ne}$  has notable consequences in the evolutionary timescales of white dwarfs. The associated energy release notably delays the cooling of white dwarfs. The precise value of the delay depends on the adopted diffusion coefficient, on the mass of the white dwarf, on the core composition, and on the possibility that white dwarfs experience a transition to a glassy state. The delay is larger for more massive white dwarfs and for carbon-rich cores. Specifically, for the case of an efficient diffusion the delay introduced in the  $1.06 M_{\odot}$  carbon-rich sequence is  $\sim 3.2$  Gyr at  $\log(L/L_{\odot}) \approx -4$ , whereas it only amounts to 0.6 Gyr in the case of the oxygen-rich sequence. In low-mass white dwarfs, appreciable delays in the cooling rates take place but only at much smaller luminosities. These results are in relatively good agreement with the results of Deloye & Bildsten (2002), although we find that the delays obtained here are somewhat larger.

To qualitatively assess the effect of  $^{22}\text{Ne}$  sedimentation on the white dwarf luminosity function, we have derived individual

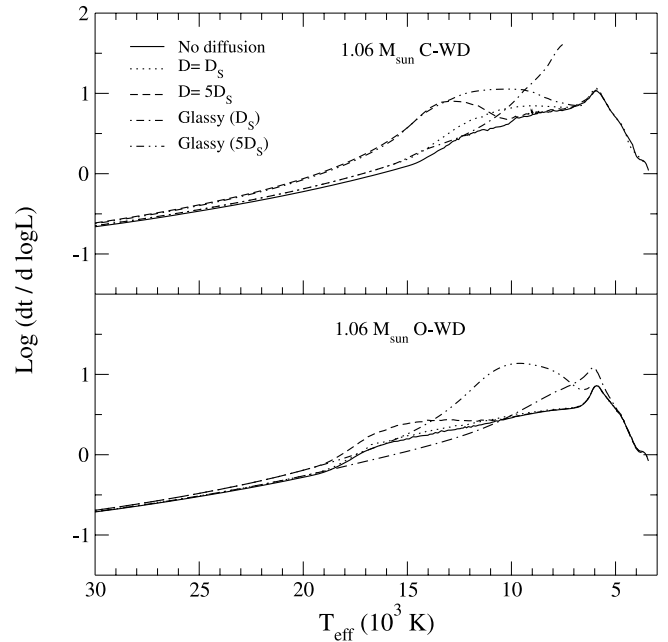


FIG. 13.—Same as Fig. 12, but results are now shown in terms of the effective temperature. The top and bottom panels show the  $1.06 M_{\odot}$  white dwarf evolutionary sequences with carbon-rich and oxygen-rich cores, respectively.

luminosity functions from our cooling curves. The number of white dwarfs of a given mass is proportional to the characteristic cooling time,  $n \propto dt/d \log(L/L_{\odot})$ . We plot this quantity in Figure 12 for the  $1.06$  and  $0.6 M_{\odot}$  white dwarf cooling sequences with carbon-rich cores as a function of the surface luminosity. The characteristic cooling times in terms of the effective temperature for the  $1.06 M_{\odot}$  white dwarf cooling sequences with carbon- and oxygen-rich cores are shown in Figure 13. In both figures, the solid line corresponds to the case in which  $^{22}\text{Ne}$  diffusion is not considered and the remaining curves to the cases of different diffusion assumptions, indicated in the figure. At large luminosities the signature of the accelerated evolution due to neutrino losses is clearly noticeable in the characteristic cooling times. At the extreme faint end of the luminosity range, the sharp decline in the luminosity function in the massive sequences reflects the onset of Debye cooling, a stage which is reached at different ages depending on the assumption about diffusion.

Note that the effect of  $^{22}\text{Ne}$  diffusion in the characteristic cooling times of low-mass white dwarfs with solar metallicity progenitors is barely noticeable. In sharp contrast, it is significant in the case of massive white dwarfs. In fact, depending on the internal composition and the uncertainties weighting on the determination of the diffusion coefficient, an increase in the number of white dwarfs by a factor of  $\approx 5$  could be expected in the effective temperature range where  $^{22}\text{Ne}$  diffusion constitutes the main source of stellar luminosity. In the case that  $D = 5D_s$  and assuming carbon-rich composition, this increase in the massive white dwarf population would be expected at  $T_{\text{eff}}$  within 12,000 and 16,000 K. For oxygen-rich cores, only a modest increase is expected at somewhat larger effective temperatures. If a transition to a glassy state is assumed instead of crystallization, a marked increase in the luminosity function is expected in both carbon- and oxygen-rich massive white dwarfs. In the case of an oxygen-rich core, this increase takes place at the effective temperature range between  $\approx 12,000$  and 8000 K. Interestingly enough, a possible large excess in the number of massive white dwarfs has been reported below  $T_{\text{eff}} = 12,000$  K (Kleinman et al. 2004;

Liebert et al. 2005; Kepler et al. 2007). Although this increase is believed to be the result of a problem in the line-fitting procedure, it might be possible that such an increase in the number of massive white dwarfs could in part be reflecting a decrease in the cooling rate of massive white dwarfs, induced by the gravitational settling of  $^{22}\text{Ne}$  in the core of these white dwarfs.

The impact of  $^{22}\text{Ne}$  sedimentation on the white dwarf structure can be assessed from pulsating white dwarfs. Indeed, as shown by Deloye & Bildsten (2002), the abundance gradient in  $^{22}\text{Ne}$  caused by diffusion in the liquid regions leaves its signature in the Brunt-Väisälä frequency which, in turn, modifies the pulsation spectrum of ZZ Ceti stars at levels compared with the uncertainties of the measurements. More interestingly, pulsating white dwarfs with measured rates of period changes can be used to assess directly the impact of  $^{22}\text{Ne}$  sedimentation on the white dwarf cooling. Indeed, the delay in the cooling times resulting from the  $^{22}\text{Ne}$  diffusion is expected to alter the rate of change of the periods of ZZ Ceti stars. For a quantitative inference of the possible impact, we write the rate of change of the pulsation period of a pulsating white dwarf as

$$\frac{\dot{P}}{P} = -a \frac{\dot{T}}{T} + b \frac{\dot{R}_*}{R_*}, \quad (21)$$

where  $T$  is the temperature of the isothermal core and  $a$  and  $b$  are constants of order unity which depend on the chemical composition, thicknesses of the hydrogen and helium envelopes, equation of state, and other ingredients involved in the modeling of white dwarfs (Winget et al. 1983). For DA white dwarfs in the ZZ Ceti instability strip, the rate of change due to gravitational

contraction, given by the second term of the right-hand side of equation (21), is usually negligible, and thus the secular rate of change of the period is directly related to the speed of cooling and is a positive contribution. The rate of secular period change has been measured for some pulsating white dwarfs. For instance, for G117-B15A, an intermediate-mass ZZ Ceti star, Kepler et al. (2005) have derived the secular variation of the main observed period of 215.2 s,  $\dot{P} = (3.57 \pm 0.82) \times 10^{-15} \text{ s s}^{-1}$ , with unprecedented accuracy. Other pulsating white dwarfs, such as L19-2 and R548, also have determinations of the secular rate of period change but are not as accurate as that of G117-B15A. We find that for the  $1.06 M_{\odot}$  carbon-rich sequence with  $D = 5D_s$  the predicted period change decreases by a factor of about 1.7, as compared with the period change in the case that diffusion is not considered. This result is very preliminary, and an in-depth study will be done in a forthcoming publication.

In summary, although the effect of the sedimentation of  $^{22}\text{Ne}$  is sizeable its impact on the white dwarf luminosity function should be minor, except for a modest increase in the derived ages, for the most reasonable assumptions. However, the imprints of the sedimentation of  $^{22}\text{Ne}$  could be detectable using pulsating white dwarfs in the appropriate effective temperature range with accurately determined rates of change of the observed periods.

Part of this work was supported by MEC grants AYA05-08013-C03-01 and 02, by European Union FEDER funds, by AGAUR, and by grant PIP 6521 from CONICET.

#### REFERENCES

- Alexander, D. R., & Ferguson, J. W. 1994, *ApJ*, 437, 879  
 Althaus, L. G., & Benvenuto, O. G. 1998, *MNRAS*, 296, 206  
 Althaus, L. G., García-Berro, E., Isern, J., & Córscico, A. H. 2005, *A&A*, 441, 689  
 Althaus, L. G., García-Berro, E., Isern, J., Córscico, A. H., & Rohrmann, R. D. 2007, *A&A*, 465, 249  
 Bedin, L. R., Salaris, M., Piotto, G., King, I. R., Anderson, J., Cassisi, S., & Momany, Y. 2005, *ApJ*, 624, L45  
 Bildsten, L., & Hall, D. M. 2001, *ApJ*, 549, L219  
 Bravo, E., Isern, J., Canal, R., & Labay, J. 1992, *A&A*, 257, 534  
 Burgers, J. M. 1969, *Flow Equations for Composite Gases* (New York: Academic)  
 Chabrier, G. 1993, *ApJ*, 414, 695  
 Deloye, C. J., & Bildsten, L. 2002, *ApJ*, 580, 1077  
 Fontaine, G., Brassard, P., & Bergeron, P. 2001, *PASP*, 113, 409  
 García-Berro, E., Hernanz, M., Isern, J., & Mochkovitch, R. 1988, *Nature*, 333, 642  
 García-Berro, E., Ritossa, C., & Iben, I., Jr. 1997, *ApJ*, 485, 765  
 Hansen, B. M. S. 2005, *ApJ*, 635, 522  
 Hansen, B. M. S., et al. 2002, *ApJ*, 574, L155  
 Hernanz, M., García-Berro, E., Isern, J., Mochkovitch, R., Segretain, L., & Chabrier, G. 1994, *ApJ*, 434, 652  
 Iben, I., Jr., & MacDonald, J. 1985, *ApJ*, 296, 540  
 Iglesias, C. A., & Rogers, F. J. 1996, *ApJ*, 464, 943  
 Isern, J., García-Berro, E., Hernanz, M., & Chabrier, G. 2000, *ApJ*, 528, 397  
 Isern, J., Mochkovitch, R., García-Berro, E., & Hernanz, M. 1991, *A&A*, 241, L29  
 ———. 1997, *ApJ*, 485, 308  
 Kalirai, J. S., Bergeron, P., Hansen, B. M. S., Kelson, D. D., Reitzel, D. B., Rich, R. M., & Richer, H. B. 2007, *ApJ*, 671, 748  
 Kepler, S. O., Kleinman, S. J., Nitta, A., Koester, D., Castanheira, B. G., Giovannini, O., Costa, A. F. M., & Althaus, L. G. 2007, *MNRAS*, 375, 1315  
 Kepler, S. O., et al. 2005, *ApJ*, 634, 1311  
 Kippenhahn, R., Thomas, H. C., & Weigert, A. 1965, *Z. Astrophys.*, 61, 241  
 Kippenhahn, R., & Weigert, A. 1990, *Stellar Structure and Evolution* (Heidelberg: Springer)  
 Kleinman, S. J., et al. 2004, *ApJ*, 607, 426  
 Lamb, D. Q., & Van Horn, H. M. 1975, *ApJ*, 200, 306  
 Liebert, J., Bergeron, P., & Holberg, J. B. 2005, *ApJS*, 156, 47  
 Mestel, L. 1952, *MNRAS*, 112, 583  
 Richer, H. B., et al. 1997, *ApJ*, 484, 741  
 Ritossa, C., García-Berro, E., & Iben, I., Jr. 1996, *ApJ*, 460, 489  
 Salaris, M., García-Berro, E., Hernanz, M., Isern, J., & Saumon, D. 2000, *ApJ*, 544, 1036  
 Segretain, L., Chabrier, G., Hernanz, M., García-Berro, E., & Isern, J. 1994, *ApJ*, 434, 641  
 Stevenson, D. J. 1980, *J. Phys. Suppl.*, 41, C61  
 Stringfellow, G. S., De Witt, H. E., & Slattery, W. L. 1990, *Phys. Rev. A*, 41, 1105  
 Van Horn, H. M. 1968, *ApJ*, 151, 227  
 Von Hippel, T., & Gilmore, G. 2000, *AJ*, 120, 1384  
 Von Hippel, T., Jefferys, W. H., Scott, J., Stein, N., Winget, D. E., DeGennaro, S., Dam, A., & Jeffery, E. J. 2006, *ApJ*, 645, 1436  
 Winget, D. E., Hansen, C. J., Liebert, J., Van Horn, H. M., Fontaine, G., Nather, R. E., Kepler, S. O., & Lamb, D. Q. 1987, *ApJ*, 315, L77  
 Winget, D. E., Hansen, C. J., & Van Horn, H. M. 1983, *Nature*, 303, 781